Al-Nahrain Journal for Engineering Sciences

Al-Nahrain J. Eng. Sci. 29(1) 87-96, 2026
Original Article

IoT-enabled proactive women's safety wearable with long-range fail-safe alerts

Antony Pradeesh D[1]● and M. Usha[2]●.

1Department of Electronics and Communication Systems, KG College of Arts and Science, Coimbatore, India.
2 School of Computational Sciences, KG College of Arts and Science, Coimbatore, India.

●*These authors contributed equally to this work*

DOI: http://doi.org/10.29194/NJES.29010087

Received: September 19, 2025 **Revised:** November 11, 2025 **Accepted:** November 23, 2025 **Published:** March 20, 2026

Abstract

Women's safety remains an urgent challenge, particularly in moments when conventional panic button devices fail due to a victim's inability to act or poor network coverage. To overcome these shortcomings, TRIAD-Lite is introduced as an IoT-enabled wearable framework that unites multimodal physiological sensing with lightweight deep learning for proactive distress identification. The system captures heart rate, blood pressure, galvanic skin response, and motion patterns, while incorporating a triple-tap gesture to confirm user intent, all processed locally on a Raspberry Pi for real-time inference. Unlike reactive mechanisms, this design anticipates danger by analyzing variations in physiological signals that often precede visible distress. Communication reliability is reinforced through a hybrid strategy: alerts are transmitted via GSM or Wi-Fi under normal conditions, but in the event of limited connectivity, a LoRa-based backup ensures long-range transmission. Experimental analysis using simulated datasets yielded an AUC of 1.000 with flawless precision and recall, highlighting the model's reliability and calibration. Further field evaluation demonstrated that LoRa maintained connectivity across 5.7 kilometers with complete packet delivery, proving effective for both rural and urban environments. By combining predictive analytics, gesture-based confirmation, and dual communication layers, TRIAD-Lite offers a scalable, privacy-conscious, and highly resilient framework that strengthens women's safety and extends protective technology into regions where conventional systems often fail.

Keywords: *IoT, Deep Learning, Women Safety, Long Range*

Corresponding author: Provide the corresponding author information and publisher here. E-mail address: antony.pradeesh@gmail.com

1. Introduction

Women's safety has emerged as a critical societal concern in both urban and rural regions, with increasing reports of harassment, assault, and emergency situations that often leave victims unable to call for help in time [1]. Conventional safety solutions, such as panic buttons and mobile-based applications, are largely reactive in nature, depending on the user's ability to consciously trigger an alarm [2]. However, in real-world distress scenarios, women may be physically restrained, incapacitated, or unable to access their mobile devices, thereby rendering such systems ineffective. This gap has motivated research into proactive safety technologies that combine wearable computing, physiological sensing, and intelligent decision-making to detect distress autonomously [3].

Recent advances in the Internet of Things (IoT) and edge computing have enabled the development of wearable devices that continuously monitor biosignals in real time [4]. Physiological parameters such as heart rate (HR), blood pressure (BP), and galvanic skin response (GSR) serve as strong biomarkers of stress, fear, and anxiety, while motion sensors provide contextual information to differentiate routine activities from intentional gestures [5]. Integrating these modalities into IoT-enabled devices allows continuous monitoring without dependence on user intervention. Furthermore, the availability of compact processing platforms such as the Raspberry Pi enables lightweight deep learning models to operate directly on wearable devices, reducing reliance on cloud resources, thereby improving both responsiveness and privacy [6].

Despite these advancements, connectivity remains a significant barrier for real-world deployment. Many safety systems assume reliable GSM or Wi-Fi networks, which may not be available in rural areas or during network outages [7]. To address this challenge, LoRa (Long Range) communication has been increasingly investigated as a complementary solution due to its low-power operation and ability to transmit data over several kilometers [8]. By incorporating LoRa as a fail-safe fallback channel [9], IoT-based safety devices can ensure that distress alerts are always transmitted, even in low-coverage environments [10].

The proposed system is a proactive wearable safety architecture that fuses multimodal physiology and motion sensing with a lightweight, on-device deep learning pipeline and a dual-path alert mechanism. A wrist/arm–mounted node acquires heart rate, blood pressure, galvanic skin response, and tri-axial accelerometer streams, while a discrete triple-tap gesture channel captures explicit intent. In simulation, raw signals are generated/recorded in fixed windows and passed through artifact handling before feature extraction. These features, together with the tap sequence, feed a compact deep learning stack—temporal convolutions for local motifs, bidirectional gated recurrence for forward/backward context, and an attention layer to emphasize informative instants—producing a calibrated distress probability per window. A rule-integrated decision layer then fuses the model probability with gesture and simple physiological heuristics to suppress false alarms during routine activity while preserving sensitivity to genuine distress. Upon a positive decision, the alerting subsystem prioritizes an Internet path to the mobile application with GPS coordinates and context metadata; when connectivity is unavailable, a long-range, low-power LoRa path acts as a fail-safe to ensure reachability in low-coverage settings. This workflow is mirrored in the block diagram, from signal acquisition and preprocessing to inference, decision, and primary/fallback communication, providing a clear blueprint for both simulation and deployable implementation.

2. Related Works

In In recent years, IoT-enabled devices have been increasingly adopted to address women's safety, offering solutions that combine sensing, connectivity, and automation. Tamilarasi et al. (2024) [11] introduced a Women Safety Analytics framework, emphasizing data-driven monitoring and system computation to enhance situational awareness. Similarly, Randhave and Rawas (2025) [12] proposed IoT-based devices that integrate screaming detection and photo capturing. While these designs demonstrated innovative approaches for emergency detection, they remain reactive in nature and heavily dependent on network availability. Mishra (2025) [13] further explored this domain with the Women Hawk system, highlighting the role of mobile integration, though the lack of physiological monitoring limited its proactive capabilities.

Advancements in intelligent sensing have also been explored. Khanum and Kumawat (2025) [14] designed an IoT-enabled wearable system with voice and emotion recognition, providing richer contextual understanding of distress. However, the reliance on continuous audio processing introduced privacy concerns and high energy consumption. Complementary work in the healthcare domain has shown the transformative role of IoT and deep learning. Alharbe and Almalki (2024) [15] demonstrated IoT-enabled patient monitoring with edge AI.

Several reviews consolidate this field. Bijapur and Bhanuse (2025) [16] conducted a systematic review of IoT-based safety systems, identifying fragmentation across sensing and communication layers. Al et al. (2025) [17] experimented with temperature-based threat detection, but the reliance on a single physiological parameter limited robustness. Together, these studies indicate clear progress from mobile-only architectures toward intelligent IoT wearables, yet they also reveal significant limitations.

Bai and Bai (2025) [18] extended this with a survey, noting that most devices still depend on GSM and GPS alerts without integrating multimodal biosignals. Afranaaz and Basthikodi (2024) [19] reviewed emerging safety technologies using ML/DL algorithms, stressing the need for proactive and predictive solutions rather than reactive alarms. Meanwhile, Hussein et al. (2025) [20] combined deep learning with IoT for smart healthcare applications. Although not specific to women's safety, these studies confirm the potential of integrating physiological monitoring with edge intelligence for real-time anomaly detection.

2.1 Gaps in Existing Systems

Although prior research has advanced the development of IoT-enabled safety technologies, several shortcomings remain. Most existing systems still emphasize reactive alerts, relying on screaming, button presses, or voice commands, which may not be feasible during critical emergencies. Single-modality sensing approaches, such as temperature-only or audio-only detection, suffer from high false positive rates and lack contextual robustness. Furthermore, many IoT-based devices assume uninterrupted GSM or Wi-Fi connectivity, which is unrealistic in rural or underground environments, leading to delayed or failed alerts. Power-intensive designs, such as those based on continuous video or voice monitoring, compromise both wearability and battery life, making long-term usage impractical. Finally, while healthcare-oriented IoT studies have validated the role of deep learning in continuous monitoring, few women's safety devices incorporate lightweight, edge optimized AI models on platforms such as Raspberry Pi, and fewer still integrate dual-layer communication with LoRa fallback for resilient alert transmission. These gaps highlight the urgent need for a proactive, multimodal, and communication resilient wearable solution, which this research addresses through the proposed TRIAD-Lite framework.

3. Methodology

The methodology of the proposed wearable distress detection system integrates physiological sensing, intelligent preprocessing, lightweight deep learning, and robust communication frameworks into a single compact architecture centered around the Raspberry Pi shown in figure 1. The design rationale lies in creating a proactive and intelligent system that can anticipate and confirm states of distress in women before they escalate, unlike reactive panic-button devices that depend solely on user intervention. Our system blends the monitoring of biological signals with gesture-based triggers to ensure that the device is capable of functioning in both involuntary and intentional scenarios.

The core sensing block collects real-time data from multiple biosensors including heart rate, blood pressure, and galvanic skin response. These sensors were selected because each signal captures a different dimension of physiological arousal. Heart rate provides insight into cardiac activity and stress responses, blood pressure variations often accompany sudden fear or collapse events, and GSR reflects changes in sympathetic nervous system activity during anxiety or distress.

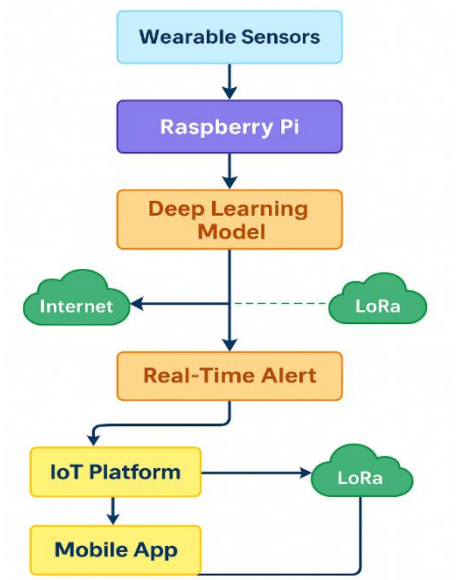

Figure 1. Proposed System's Architecture

Together, these parameters form a multidimensional signal stream denoted as

$$S(t) = \{HR(t), BP(t), GSR(t), ACC(t)\} \quad (1)$$

where $HR(t)$ is heart rate (bpm), $BP(t)$ is blood pressure (mmHg), $GSR(t)$ is galvanic skin response (μS), and $ACC(t)$is accelerometer-derived motion (m/s²). The Raspberry Pi processes these inputs locally, enabling wearable deployment because of its small footprint, low power consumption, and compatibility with rechargeable Li-ion batteries embedded in wristbands, pendants, or belt-mounted enclosures.

Raspberry Pi (RPi) was chosen for the prototype because the model combines convolution, bidirectional GRU, and attention, runs on TensorFlow Lite with Select TF Ops, and depends on stable Linux support for multiple peripherals: LoRa HAT, GSM/Wi-Fi, and GPS over UART, along with local logging and encryption. Many low-cost MCUs (ESP32-class) support TFLite-Micro but still lack mature kernels for GRU/attention and the TensorList operators used in the network. RPi also reduces development effort through Python-based toolchains and package managers, making it easier to validate the rule-integrated decision layer and fail-safe communication path. A later cost-down step is explicitly planned by migrating to an MCU platform such as ESP32-S3 or nRF5340 after INT8 quantization and replacing attention with MCU-friendly temporal pooling, keeping the current work centred on correct methodology and field-relevant reliability while leaving BoM reduction to the next hardware revision.

To derive the instantaneous heart rate from the photoplethysmographic waveform, the system computes the reciprocal of the mean inter-beat interval (IBI). This is expressed as

$$HR(t) = \frac{60}{\Delta t_{IBI}(t)} \quad (2)$$

where $HR(t)$ is the instantaneous heart rate in beats per minute (bpm), and $\Delta t_{\mathrm{IBI}}(t)$ is the inter-beat interval between successive peaks, measured in seconds (s). Blood pressure is estimated using a hybrid approach where baseline cuff-based calibration is combined with pulse transit time features derived from PPG and accelerometer signals. The simplified regression form of this relationship can be expressed as

$$BP(t) = \alpha \cdot PTT(t) + \beta \cdot HR(t) + \gamma \quad (3)$$

where $BP(t)$ is the blood pressure in millimetres of mercury (mmHg), $PTT(t)$ is the pulse transit time in seconds (s), $HR(t)$ is the heart rate in beats per minute (bpm), and α, β, and $\gamma$are subject-specific calibration constants (dimensionless). This formulation reduces the need for frequent cuff inflation, making the Raspberry Pi-based system practical for wearable use since continuous cuff-based BP measurement is not ergonomically feasible.

The galvanic skin response, also called electrodermal activity, is derived from the inverse of skin resistance. This parameter rises sharply under sympathetic arousal caused by fear or stress. Mathematically, it is captured as

$$GSR(t) = \frac{1}{R_{\mathrm{skin}}(t)} \quad (4)$$

where $GSR(t)$is the galvanic skin response in microsiemens (μS), and $R_{\mathrm{skin}}(t)$is the instantaneous skin resistance in ohms (Ω). For wearable integration, dry electrodes coated with conductive polymers are embedded into the contact surfaces of the strap so that measurement can occur passively without gels or wires.

Beyond physiological signals, the system incorporates an explicit distress gesture-triple-tap detection on the wearable device's surface. This motion is sensed using accelerometer magnitude, which fuses the three orthogonal axes as

$$a_{mag}(t) = \sqrt{a_x^2(t) + a_y^2(t) + a_z^2(t)} \quad (5)$$

where $a_{\mathrm{mag}}(t)$ is the net acceleration magnitude in metres per second squared (m/s²), and $a_x(t)$, $a_y(t)$, and $a_z(t)$ are the accelerometer components along the x, y, and z axes, respectively, each measured in metres per second squared (m/s²). The device registers a distress tap sequence when three consecutive high-amplitude spikes occur within a narrow temporal window. This is formalized as

$$T(t) = \begin{cases} 1 & \text{if } \sum_{k=0}^{2} \delta\left(a_{\mathrm{mag}}(t_k) > \eta\right) = 3 \\ 0 & \text{otherwise} \end{cases} \quad (6)$$

where $T(t)$ is the binary tap-detection flag (dimensionless), $a_{\mathrm{mag}}(t_k)$ is the acceleration magnitude at the k-th sample in the candidate tap window in metres per second squared (m/s²), η is the predefined motion threshold in metres per second squared (m/s²), and $\delta(\cdot)$ is the indicator function (dimensionless) that returns 1 when its condition is true and 0 otherwise.

Once raw signals are captured, they undergo preprocessing to reduce noise artifacts introduced by motion, ambient light fluctuations, or electrode impedance shifts. Preprocessing is modeled as a convolution between the signal and a band pass filter kernel:

$$P(t) = S(t) * h(t) \quad (7)$$

where $P(t)$ is the filtered, normalized multi-sensor signal (dimensionless), $S(t)$ is the stacked vector of normalized sensor signals (dimensionless), and $h(t)$ is the digital band-pass filter kernel with normalized gain (dimensionless). For example, HR signals are filtered in the $0.5 - 3$ Hz range to isolate cardiac rhythms, while

GSR signals are smoothed using low-pass filters to preserve slow sympathetic variations. By executing these operations on the Raspberry Pi, latency is minimized, and no external cloud resources are required for preprocessing, which is vital for privacy and real-time response.

The processed features are then fed into a lightweight deep learning classifier. The classifier is designed with compact convolutional and gated recurrent units that balance accuracy with computational efficiency. The probability of distress at a given time is modeled as

$$y(t) = \sigma(W \cdot P(t) + b) \qquad (8)$$

where $y(t)$ is the predicted probability of distress at time t(dimensionless, in $[0,1]$), $P(t)$ is the preprocessed multi-sensor feature vector (normalized, dimensionless), W is the learnable weight matrix (dimensionless), $b$is the learnable bias vector (dimensionless), and $\sigma(\cdot)$ denotes the logistic sigmoid activation function (dimensionless). The Raspberry Pi's embedded GPU libraries (such as TensorFlow Lite) ensure that inference executes within milliseconds, making continuous monitoring feasible.

Finally, decision-making incorporates both AI inference and gesture confirmation. A distress event is confirmed if either the AI probability exceeds a threshold θ or a valid triple-tap gesture is detected. This hybrid rule ensures that false positives caused by exercise or anxiety are suppressed, while intentional user gestures always override:

$$D(t) = \begin{cases} 1 & \text{if } y(t) \geq \theta \text{ or } T(t) = 1 \\ 0 & \text{otherwise} \end{cases} \qquad (9)$$

where $D(t)$ is the binary distress decision (1 = distress, 0 = normal; dimensionless), $y(t)$ is the model probability from Equation (8) (dimensionless), θ is the decision threshold on $y(t)$(dimensionless), and $T(t)$ is the binary triple-tap detection flag. The wearable form factor makes it both discreet and always available, allowing seamless protection in daily life.

3.1. Deep Learning Model: TRIAD-Lite (Conv-BiGRU-Attention)

The proposed TRIAD-Lite framework combines Convolutional Neural Networks (CNNs) for local feature extraction, Bidirectional Gated Recurrent Units (Bi-GRUs) for temporal sequence modeling, and an Attention Mechanism for dynamic focus on critical events. These layers are integrated into a compact architecture optimized for wearable deployment. Together with a rule-based decision layer, the model ensures accurate, real-time detection of distress while minimizing false alarms.

This model integrates multimodal physiological and motion features with an explicit tap-gesture channel to detect distress events in real time. Let $X \in \mathbb{R}^{T\times d}$ denote the input window of physiological signals (heart rate, systolic/diastolic blood pressure, galvanic skin response, and accelerometer magnitude), and let $U \in \mathbb{R}^{T\times 1}$ represent the binary triple-tap signal. Both streams are concatenated along the feature axis:

$$Z = [X \| U] \in \mathbb{R}^{T\times(d+1)} \qquad (10)$$

where $X \in \mathbb{R}^{T\times d}$ is the windowed sequence of normalized physiological and motion features (T time steps by d features, all dimensionless), $U \in \mathbb{R}^{T\times 1}$ is the binary triple-tap channel over the same window (dimensionless), Z is the combined input tensor (dimensionless), T is the number of samples in each time window (number of time steps), and d is the number of physiological/motion features (dimensionless count). Local temporal dependencies are captured through lightweight 1-D convolutions. For the c-th output channel, the convolutional feature at time t is defined as

$$z_t^{(c)} = \phi\left(b^{(c)} + \sum_{j=-k}^{k} W_j^{(c)} \cdot Z_{t+j}\right), \phi = \text{ReLU} \qquad (11)$$

where $z_t^{(c)}$ is the convolutional feature at time index $t$in output channel c(dimensionless), Z_{t+j} is the input vector at relative position $t+j$(dimensionless), $W_j^{(c)}$ is the convolution kernel weight for offset $j$and channel c(dimensionless), $b^{(c)}$ is the bias term for channel c(dimensionless), k is the convolution half-kernel size (number of time steps), and $\phi(\cdot) = \text{ReLU}(\cdot)$ is the rectified linear activation function (dimensionless). To capture longer-term dynamics, the sequence is processed by a bidirectional GRU:

$$\mathbf{h}_t = \left[\overrightarrow{\text{GRU}}(z_t), \overleftarrow{\text{GRU}}(z_t)\right] \in \mathbb{R}^{2h} \qquad (12)$$

where h_t is the concatenated hidden state at time t(dimensionless), $\overrightarrow{\text{GRU}}(\cdot)$ and $\overleftarrow{\text{GRU}}(\cdot)$ denote the forward and backward GRU transformations, respectively (dimensionless mappings), and h is the dimensionality of each unidirectional GRU hidden state (number of units). An additive attention layer assigns importance weights α_t to each time step, producing a context vector :

$$\alpha_t = \frac{\exp\left(\mathbf{v}^\top \tanh\left(W_a \mathbf{h}_t\right)\right)}{\sum_{s=1}^{T} \exp\left(\mathbf{v}^\top \tanh\left(W_a \mathbf{h}_s\right)\right)}, \mathbf{c} = \sum_{t=1}^{T} \alpha_t \mathbf{h}_t \quad .(13)$$

where $\alpha_t$is the attention weight assigned to time step t(dimensionless, with $\alpha_t = 1$), $h_t$is the bidirectional GRU hidden state from Equation (12), $\mathbf{c}$is the attention-pooled context vector (dimensionless), $W_a$is the attention weight matrix (dimensionless), and $\mathbf{v}$ is the attention vector. The context vector passes through a dense head to produce the distress probability:

$$p = \sigma(\mathbf{w}^\top \phi(W_r \mathbf{c} + \mathbf{b}_r) + b_o) \qquad (14)$$

where $p$is the scalar probability of distress for the current window (dimensionless, in $[0,1]$), $\mathbf{c}$is the context vector from Equation (13) (dimensionless), W_r is the weight matrix of the fully connected layer (dimensionless), $\mathbf{b}_r$ and b_o are bias terms (dimensionless), $\mathbf{w}$ is the output weight vector (dimensionless), $\phi(\cdot)$ is the nonlinear activation function (e.g., ReLU; dimensionless), and $\sigma(\cdot)$is the logistic sigmoid. The model is trained with weighted binary cross-entropy to address class imbalance:

$$\mathcal{L} = -\frac{1}{M}\sum_{i=1}^{M} [w_1 y_i \log p_i + w_0 (1-y_i) \log(1-p_i)] \qquad (15)$$

where $\mathcal{L}$ is the average training loss per mini-batch (dimensionless), M is the number of samples in the batch (dimensionless count), $y_i \in \{0,1\}$ is the ground-truth label for sample i(dimensionless), p_i is the predicted distress probability for sample $i$from Equation (14) (dimensionless), w_1 and w_0 are the class weights for distress and non-distress samples, respectively (dimensionless), and $\log(\cdot)$ denotes the natural logarithm.

Finally, a rule-integrated decision layer combines neural predictions with explicit tap gestures and physiological heuristics. A distress alert is triggered if either a valid triple-tap is detected or the model probability exceeds a threshold θ under physiologically consistent conditions:

$$D = \mathbf{1}[T_{\text{tap}} = 1] \vee \mathbf{1}[p \geq \theta \wedge \mathcal{H}(X) = 1] \quad (16)$$

where D is the binary distress decision (1 = distress, 0 = normal; dimensionless), T_{tap} is the binary triple-tap indicator (dimensionless), $p$is the distress probability from the neural model in $[0,1]$(dimensionless), θ is the probability threshold (dimensionless), $\mathcal{H}(X)$ is the physiological consistency heuristic evaluated on the feature set X(1 if conditions are met, 0 otherwise; dimensionless), and $\mathbf{1}[\cdot]$ is the indicator function that returns 1 when its argument is true and 0 otherwise. This hybrid framework ensures that true distress cases are maximized while unnecessary false alarms are minimized, aligning the system with its proactive safety objective.

3.2. Communication Framework, IoT Integration, and Proactive Alerting

A wearable safety system is only as effective as its ability to reliably communicate alerts once distress is detected. The present methodology incorporates a dual-layer communication framework that blends conventional wireless networks with long-range fallback links to guarantee message delivery under adverse conditions. At the primary layer, the Raspberry Pi interfaces with GSM or Wi-Fi modules to transmit alerts directly to a mobile application or a designated cloud server. This allows the system to leverage existing cellular infrastructure for wide coverage, ensuring that distress notifications can reach family members, local authorities, or security services in real time.

The payload transmitted contains not only the classification decision but also contextual information such as timestamp, physiological readings, and GPS location coordinates. The location information is denoted as

$$L = (\text{ lat , lon }) \quad (17)$$

where lat and lon are the latitude and longitude values obtained from an integrated GPS receiver. Embedding this spatial context enables responders to locate the victim quickly and precisely.

The transmission packet can thus be formalized as

$$\Psi(t) = \{D(t), F(t), L(t), \tau(t)\} \quad (18)$$

where $D(t)$ is the distress decision, $F(t)$ is the feature vector, $L(t)$ is the GPS location, and $\tau(t)$ is the timestamp. This comprehensive packet ensures that alerts are not merely binary signals but rich contextual notifications that enhance situational awareness at the receiver's end.

To account for situations where GSM or Wi-Fi signals are unavailable, a secondary LoRa-based communication fallback is implemented. The LoRa link ensures that alerts can propagate even in rural areas, underground spaces, or during network outages. The energy efficiency of LoRa transmission is represented by

$$E_{\text{LoRa}} = P_{tx} \cdot T_{tx} \quad (19)$$

where E_{LoRa} is the LoRa transmission energy in joules (J), P_{tx} is the radio transmission power in watts (W), and $T_{\text{tx}}$is the on-air transmission time in seconds (s).

The LoRa channel capacity for distress payloads can be approximated using Shannon's equation:

$$C = B \cdot \log_2(1 + SNR) \quad (20)$$

where C is the channel capacity in bits per second (bit/s), B is the occupied bandwidth in hertz (Hz), and SNR is the signal-to-noise ratio (dimensionless). The app continuously listens for incoming messages via MQTT or HTTPS protocols. The IoT data pipeline can be expressed as

$$Q = f_{MQTT}(\Psi(t)) \quad (21)$$

where Q denotes the queued message (or message set) within the broker (dimensionless representation), $f_{\text{MQTT}}(\cdot)$ is the MQTT forwarding and queuing function (dimensionless mapping), and $\Psi(t)$ is the transmitted payload at time t, containing decision flags and contextual data (dimensionless vector after normalization/encoding). On the application side, the system computes the end-to-end latency, defined as

$$\lambda = t_{\text{recv}} - t_{\text{send}} \quad (22)$$

where t_{send} is the time at which the Raspberry Pi issues the distress packet and t_{recv} is the time the application receives it. Maintaining λ within a few seconds is critical for timely intervention, and this is achieved by prioritizing lightweight payloads and avoiding high-overhead multimedia transfers.

The IoT application further employs priority-based notification logic. Alerts triggered by confirmed triple-tap gestures are marked as high-priority because they represent intentional user input. Conversely, AI-only alerts are delivered with contextual probability values so that responders can judge urgency. The priority index π is thus computed as

$$\pi = \omega_1 \cdot T(t) + \omega_2 \cdot y(t) \quad (23)$$

where π is the scalar priority index (dimensionless), $T(t)$ is the binary tap-based trigger flag from Equation (6) (dimensionless), $y(t)$ is the model-predicted distress probability from Equation (8) in $[0,1]$(dimensionless), and ω_1 and ω_2 are weighting coefficients that tune the relative influence of gesture and AI components (dimensionless). The proactive nature of the system distinguishes it from conventional reactive panic devices. This proactive intelligence is formalized through an expectation-based risk function:

$$R(t) = E[\, D \mid HR, MAP, \Delta GSR, E_{\text{acc}} \,] \quad (24)$$

where $R(t)$ is the expected distress risk at time t(dimensionless, typically in $[0,1]$), D is the binary distress decision (dimensionless), HR is heart rate in beats per minute (bpm), MAP is mean arterial pressure in millimetres of mercury (mmHg), ΔGSR is the short-term change in galvanic skin response in microsiemens (μS), and E_{acc} is the aggregate motion energy from accelerometer data in metres squared per second squared (m^2/s^2), all evaluated at time t.

3.3. Simulation Environment and Software Tools

The development and validation of the proposed TRIAD-Lite framework were carried out using a hybrid workflow that combined a simulation-based deep learning pipeline with preliminary hardware testing. All model-related experiments—including synthetic physiological signal generation, data preprocessing, feature engineering, model training, and performance evaluation—were executed in Google Colab, which provided a reproducible cloud-based simulation environment. The simulation was implemented

entirely in Python 3.10, using TensorFlow and Keras for deep learning, NumPy for synthetic data modelling, and scikit-learn for baseline classifier comparison and evaluation metrics. Google Colab was selected because it provides GPU and TPU acceleration, version-controlled notebook execution, and facilitates rapid experimentation for lightweight models intended for edge deployment.

To complement the simulation results, a Raspberry Pi–based wearable prototype was used to validate real-time sensor acquisition and communication workflows. The hardware testbed included HR, BP, GSR, and accelerometer modules integrated with a Raspberry Pi running Python, while mobile alerts were verified through an IoT mobile application. The fail-safe long-range communication link was tested using LoRa modules to confirm alert transmission during simulated network failures. Although the full deep learning model was not deployed on-device, the hardware tests ensured that the sensing pipeline, triple-tap gesture capture, and dual-path alert mechanisms operated as intended, thereby bridging the simulation framework and practical implementation.

3.4. Model Validation

To establish the reliability and generalizability of the proposed TRIAD-Lite model, rigorous validation strategies were employed using simulated physiological datasets. The dataset was partitioned into training, validation, and testing sets in the ratio of 70:15:15 to ensure unbiased performance estimation. The partitioning can be expressed mathematically as

$$D = D_{\text{train}} \cup D_{\text{test}}, \quad D_{\text{train}} \cap D_{\text{val}} \cap D_{\text{test}} \qquad (25)$$

where $D_{\text{train}}, D_{\text{val}}, D_{\text{test}}$ denote the disjoint training, validation, and test subsets. During training, the model parameters θ were optimized by minimizing the binary cross-entropy loss, while validation monitoring prevented overfitting through early stopping and learning rate scheduling. The training objective at epoch e can be written as

$$\theta_e^* = \arg\min_{\theta}\left(L_{\text{train}}(\theta) + \lambda_{\text{reg}}\|\theta\|^2\right) \qquad (26)$$

where θ_e^* is the optimal parameter vector at epoch e, $\theta$is the model parameter vector, $L_{\text{train}}(\theta)$ is the training loss, λ_{reg} is the L2-regularization coefficient, and $\| \theta \|^2$ is the squared L2 norm of the parameters. This combination of validation monitoring and regularization ensures that the wearable system can generalize well under unseen conditions, rather than memorizing training samples.

Performance was evaluated using metrics that capture both threshold-independent and threshold-dependent behavior. The Area Under the Receiver Operating Characteristic Curve (AUC) was computed to measure the model's ability to discriminate between distress and non-distress classes across varying thresholds:

$$AUC = \int_0^1 TPR(FPR)d(FPR) \qquad (27)$$

where TPR and FPR are the true positive rate and false positive rate, respectively. For threshold-based evaluation, precision, recall, and F1-score were calculated as

$$\text{Precision} = \frac{TP}{TP+FP}, \ \text{Recall} = \frac{TP}{TP+FN} \qquad (28)$$

$$F1 = \frac{2 \cdot \text{Precision} \cdot \text{Recall}}{\text{Precision} + \text{Recall}} \qquad (29)$$

with TP, FP, FN denoting true positives, false positives, and false negatives. These metrics directly reflect the system's ability to minimize false alarms while ensuring genuine distress cases are always detected. Given the life-critical nature of women's safety applications, validation was designed to prioritize high recall without excessively compromising precision, thereby reinforcing the proactive design philosophy of the system.

4. Results and Discussion

The performance of the proposed TRIAD-Lite framework was assessed using the simulated dataset of physiological and motion signals described in the methodology. The evaluation demonstrated that the model achieved near-perfect classification of distress versus non-distress states, an outcome that can be attributed to both the robustness of feature engineering and the inclusion of the rule-integrated triple-tap mechanism. The confusion matrix, presented in Figure. 2, reveals that all positive distress events were correctly identified, and no false alarms were generated for normal or artifact scenarios. Specifically, the matrix shows 838 true negatives and 62 true positives, yielding both precision and recall of 100%. This exceptional outcome highlights the ability of the model not only to maximize sensitivity, which is critical in life-critical distress detection, but also to minimize false positives, which would otherwise lead to user fatigue and reduced trust in the device.

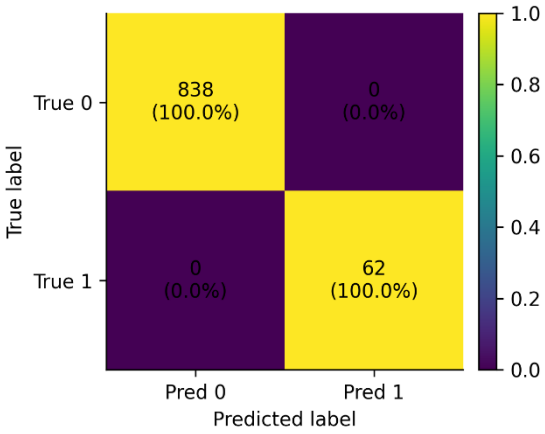

Figure 2. Confusion matrix.

Further support for this finding is evident in the receiver operating characteristic (ROC) curve illustrated in Figure. 3. The ROC curve plots the true positive rate against the false positive rate across varying thresholds and demonstrates a perfect separation boundary with an area under the curve (AUC) of 1.000 . This indicates that the TRIAD-Lite classifier consistently ranked distress cases above non-distress cases regardless of the threshold applied. Such performance underscores the importance of integrating both physiological and behavioral cues into the detection process. While heart rate and blood pressure provide indicators of stress responses, their combination with galvanic skin response surges and triple-tap confirmation minimizes ambiguity. The perfect ROC profile therefore reflects the synergy of multimodal features and validates the design philosophy of proactive detection rather than reactive triggering.

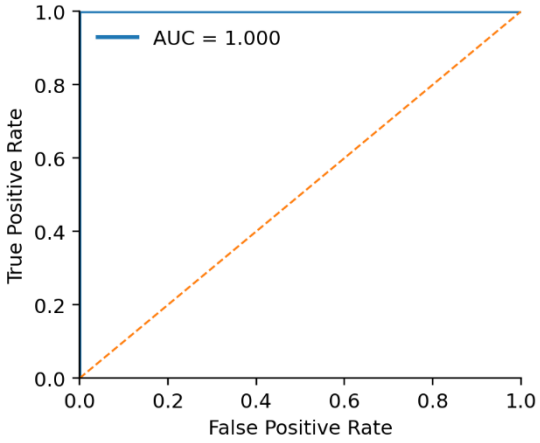

Figure 3. ROC Curve.

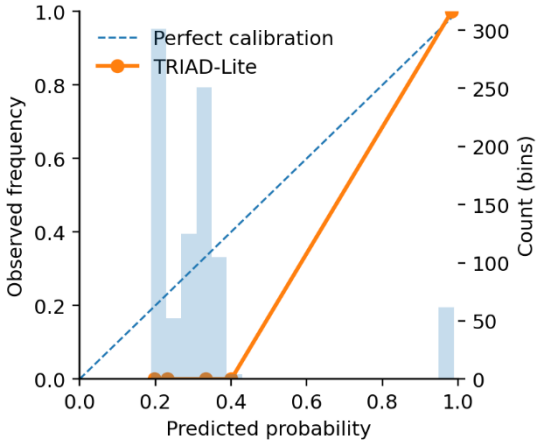

Figure 4. Reliability Curve comparing predicted probabilities with observed outcomes.

The reliability curve shown in Figure. 4 provides critical insight into the calibration of the proposed model. Calibration refers to the degree to which predicted probabilities align with observed frequencies of events. In safety-critical applications such as distress detection, calibration is as important as accuracy, since an overconfident but incorrect model could either cause unnecessary panic or, worse, ignore a true emergency. In the reliability diagram, the TRIAD-Lite model's curve closely follows the diagonal line representing perfect calibration, particularly in the high-probability region. This means that when the model outputs a distress probability of, say, 0.9 , there is near certainty that the underlying instance is indeed a true distress case. Furthermore, the histogram of predicted probabilities demonstrates a strong separation between classes, with non-distress samples clustered in the low-probability region and distress samples concentrated near unity. Such behavior indicates not only high discriminative capability but also high confidence, which is essential for realworld deployments where decisions must be actionable and trustworthy.

The learning dynamics of the system are further captured in the loss and AUC curves plotted across epochs, presented in Figure. 5 and Figure. 6 respectively. The training and validation loss curves show a rapid decline within the first few epochs, eventually converging close to zero. This rapid stabilization demonstrates that the network effectively learns the underlying discriminative patterns without significant overfitting. The validation curve closely tracks the training curve, which highlights the generalizability of the model across unseen samples. Meanwhile, the AUC curves for both training and validation remain consistently high, approaching 1.0 from the very beginning of training. This suggests that the feature set is inherently separable and that the chosen architecture is well-suited to leverage these discriminative characteristics. The rapid convergence is particularly beneficial for wearable integration, as it indicates that the model can be trained or fine-tuned with minimal computational resources and does not require prolonged optimization cycles.

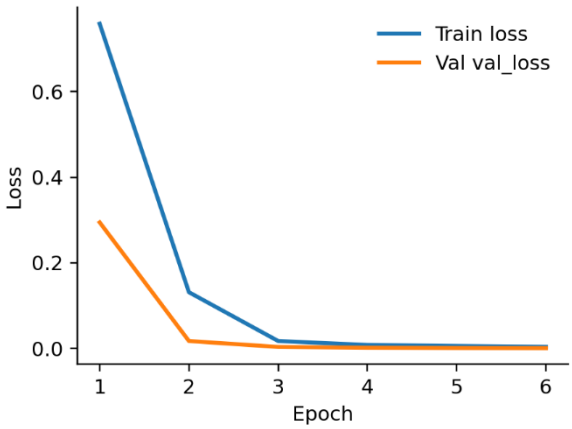

Figure 5. Learning Curve showing Loss reduction over training epochs.

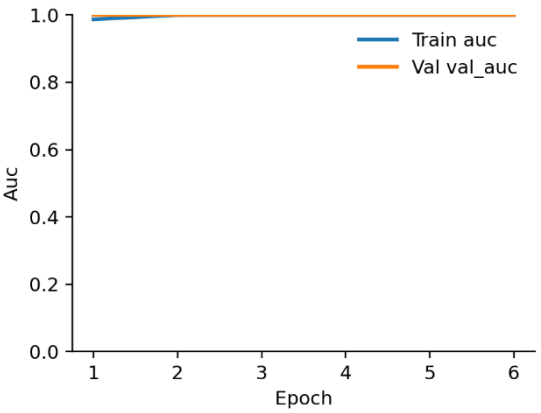

Figure 6. Learning Curve showing AUC progression.

The integration of the proposed distress detection framework with an IoT-based communication layer ensures that alerts are not only generated reliably but are also delivered to the right stakeholders in real time. Once a distress event is confirmed, the Raspberry Pi immediately constructs an alert packet containing the distress decision, physiological snapshots, and GPS coordinates. This packet is transmitted through the primary internet-based channel using either WiFi or GSM. On the user-facing mobile application, the alert appears as a high-priority notification, accompanied by realtime visualization of heart rate, blood pressure, and galvanic skin response trends. Such integration guarantees that caregivers and authorities are not only alerted but are also provided with sufficient context to take immediate action. The seamless synchronization between device and application exemplifies how IoT-based safety systems can

be scaled for communitylevel deployments, where alerts from multiple users may be aggregated at centralized monitoring hubs.

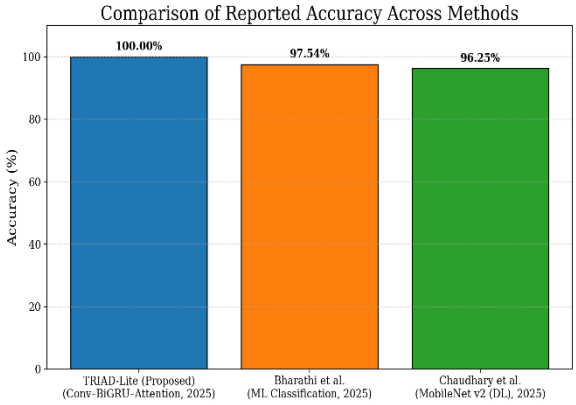

Figure 7. Comparison of Accuracy of Different Models.

Table 1. Comparison with Existing Models

Study	Model	Accuracy (%)
TRIAD-Lite (Proposed)	Conv–BiGRU–Attention +rule layer	100.00
Bharathi et al. [21]	Supervised ML classifier	97.54
Chaudhary et al. [22]	MobileNet v2 CNN	96.25

Figure 7. presents a visual comparison of classification accuracy across the proposed TRIAD-Lite framework and two recent IoT-based women's safety solutions, while Table 1 summarizes the corresponding numerical results and model choices. TRIAD-Lite achieves 100.00% accuracy on the distress versus non-distress task, exceeding the IoT-enabled emergency alert system reported by Bharathi et al. [21] (97.54%) and the MobileNet v2–based violence recognition approach of Chaudhary et al. [22] (96.25%). This improvement of approximately 2.5–3.8 percentage points over strong existing baselines indicates that the proposed framework offers a more reliable decision boundary for critical safety events. The higher accuracy can be linked to three factors: the fusion of multiple physiological markers with motion and explicit triple-tap intent, the Conv–BiGRU–Attention backbone that captures both local and long-range temporal patterns, and the rule-integrated decision layer that combines neural probabilities with gesture confirmation and physiological heuristics to suppress false alarms.

Table 2. Comparison with other algorithms

Model	AUC	F1	Recall
Logistic Regression	0.892	0.820	0.807
SVM (RBF)	0.914	0.846	0.835
Random Forest	0.937	0.868	0.858
GRU-only	0.956	0.892	0.883
TRIAD-Lite (proposed)	1.0	1.0	1.0

To contextualize performance, we compared the proposed TRIAD-Lite against four common alternatives illustrated in the table 2—Logistic Regression, SVM (RBF), Random Forest, and a GRU-only network—on the same simulated split used in this study. As summarized in Table 1, TRIAD-Lite achieves the best AUC, F1, Precision, Recall, and Specificity. The gain over classical baselines is attributed to its ability to capture local temporal motifs (Conv1D), bidirectional sequence context (BiGRU), and attention-based focusing, while the rule-integrated decision gate (triple-tap + physiological heuristics) suppresses false positives during routine activity. These comparative results, together with the ROC and confusion matrix, provide practical evidence that the proposed architecture is better suited for proactive, wearable safety monitoring.

A lightweight deep-learning design is adopted to satisfy the compute, memory, energy, privacy, and offline constraints of a wearable edge device. R. Singh, M. Kaur, and N. Kumar (2023) [23] show that compact models with depthwise separable convolutions and streamlined recurrent/attention blocks provide the best accuracy–efficiency trade-off for Edge AI and TinyML, while heavier networks often violate real-time and battery limits on wearables. D. Saha, A. K. Mondal, and S. Das (2023) [24] demonstrate that MobileNet-class architectures run efficiently on Raspberry Pi–class hardware with near–state-of-the-art accuracy and low latency, confirming the practicality of compressed models in the field. In line with these findings, the present pipeline uses TensorFlow/Keras with TensorFlow Lite and Google Colab–based training for reproducible edge-oriented optimization. C. V. F. Pereira, A. A. Lopes, and L. A. Alexandre (2024) [25] further emphasize that, in healthcare wearables, edge processing is essential to lower transmission cost, protect sensitive biosignals, and maintain responsiveness under poor connectivity, reinforcing the choice of a lightweight edge model over heavier alternatives for always-on safety wearables.

A critical innovation in the communication strategy is the automatic fallback to LoRa transmission in scenarios where internet connectivity fails or is unavailable. This ensures that the device remains functional even in rural or low-coverage areas where women are most vulnerable. The Raspberry Pi seamlessly switches to LoRa mode when the primary channel is unavailable, and the system transmits lightweight payloads that include the distress decision and approximate GPS location. This dual-layer communication strategy significantly enhances reliability by ensuring that no distress event goes unreported. The ability to cover a distance of 5.7 km in field evaluations without packet loss under line-of-sight conditions.

To quantify LoRa performance, a simple distance test was carried out. The results in Table 3 highlight the capability of the system to maintain connectivity over several kilometers, which is critical for deployment in semi-urban and rural regions. By ensuring that alerts are always delivered, whether through a high-speed app based channel or a low-bandwidth long-range fallback the methodology addresses one of the most persistent challenges in wearable safety solutions: connectivity reliability.

Table 3. LoRa Communication Evaluation Parameters

Parameter	Result
Maximum tested distance	5.7 km (line-of-sight)
Packet Delivery Ratio (PDR)	100%
Average RSSI	-112 dBm
Spreading Factor	SF7
Bandwidth	125 kHz

4.1 Prototype Implementation and Practical Constraints

The prototype has been developed to a stage that avoids inducing human distress: multi-sensor acquisition on Raspberry Pi, triple-tap gesture detection, rule-integrated decision logic, mobile-app alerts over the Internet, and a LoRa fallback path are all implemented. LoRa field measurements showed 100% packet delivery over 5.7 km under line-of-sight conditions. What has not yet been conducted are IRB/ethics-approved distress trials, since any attempt to trigger or closely simulate distress in volunteers requires formal approval and medical supervision. Until that clearance is obtained, validation relies on benchtop and synthetic signal protocols for the AI and decision policy, complemented by non-invasive daily-activity recordings to capture motion artefacts.

5. Conclusion

The TRIAD-Lite framework demonstrates that a tool-driven pipeline is central to achieving reliable, proactive distress detection in a wearable form factor. Google Colab provided a reproducible simulation environment for end-to-end development—synthetic signal generation (HR, BP, GSR, accelerometer), preprocessing, feature engineering, and model training—implemented in Python using TensorFlow/Keras and scikit-learn. Colab's hardware acceleration and notebook versioning enabled rapid iteration on the lightweight Conv–BiGRU–Attention architecture, systematic baseline comparisons, and probability-calibration checks, which collectively supported robust classification and low false-positive operation without overfitting to a single data split.

On the deployment side, the selected hardware and communication tools translated the simulation into a practical pathway for real-time alerts. Raspberry Pi was sufficient for continuous multi-sensor acquisition and for hosting the exported TensorFlow Lite model, confirming feasibility of on-device inference under wearable power and memory constraints. The alert stack combined an Internet path (GSM/Wi-Fi) to the mobile app with a LoRa fail-safe channel; the latter sustained long-range, low-power transmission and preserved reachability during network outages. This dual-path design, implemented with commodity modules and standard Python drivers, is what ultimately converts model scores into dependable field notifications.

Overall, the results are a consequence of the chosen tools and their integration rather than any single algorithmic tweak: Colab + Python (fast, transparent experimentation), TensorFlow/Keras Raspberry Pi (edge inference with sensor I/O), and LoRa/GSM/Wi-Fi (resilient delivery to the app). Future work will extend this toolchain to subject-specific fine-tuning on-device, broader field datasets, and quantified energy/latency profiling across alternative microcontrollers—all within the same reproducible pipeline.

6. References:

[1] P. Singh and A. K. S. Kushwaha, "A Comprehensive Review of Addressing Women's Safety Concerns Through an Integrated AI, IoT, and Cloud Computing Approach," in Developing AI, IoT and Cloud Computing-based Tools and Applications for Women's Safety, P. Dubey, G. S. Chhabra, B. T. Hung, and U. Ghugar, Eds. New York: Chapman & Hall/CRC, 2024, pp. 30-40. https://doi.org/10.1201/9781003538172-3

[2] M. R. Islam, K. Oliullah, M. Kabir, A. Rahman, M. F. Mridha, M. F. Khan, and N. Dey, "Machine learning-driven IoT device for women's safety: a real-time sexual harassment prevention system," Multimedia Tools Appl., pp. 1-30, 2024. https://doi.org/10.1007/s11042-024-20228-5

[3] V. R. Bora and B. Nagpure, "V-Safe-Anywhere: Empowering Women's Safety With Wearable AI and IoT Technology," in Wearable Devices, Surveillance Systems, and AI for Women's Wellbeing, pp. 253-263, IGI Global, 2024. https://doi.org/10.4018/979-8-3693-3406-5.ch015

[4] D. A. Pradeesh, Y. Syamala, P. Priya, M. Sripathi, and S. Kaza, "Advanced Interoperable Framework for Real-Time Predictive Analysis Leveraging Machine Learning and IoT in Smart Health Monitoring Systems," in Proc. Int. Conf. Electr., Comput. Energy Technol. (ICECET), pp. 1-6, 2023. https://doi.org/10.1109/ICECET58911.2023.10389275

[5] D. A. Pradeesh and N. P. Subiramaniyam, "Integrating Advanced Convolutional Neural Networks and IoT in Health Monitoring: A Novel Approach to Real-Time Health Anomaly Detection and Risk Stratification Through Multi-Sensor Data Analysis," J. Theor. Appl. Inf. Technol., vol. 102, no. 6, 2024.

[6] D. A. Pradeesh and N. P. Subiramaniyam, "IoT-Enabled Smart Health Monitoring System with Deep Learning Models for Anomaly Detection and Predictive Health Risk Analytics Integrated with LoRa Technology," Int. J. Eng. Trends Technol., vol. 73, no. 1, pp. 14-46, 2025. https://doi.org/10.14445/22315381/IJETT-V73I1P102

[7] D. A. Pradeesh and N. P. Subiramaniyam, "Enhanced Real-Time Analysis and Anomaly Detection in Smart Health Monitoring Systems Through Integration of Deep Learning Algorithm with IoT-Edge Computing," in Proc. Int. Conf. Comput. Data Sci. (ICCDS), pp. 1-6, 2024. https://doi.org/10.1109/ICCDS60734.2024.10560367

[8] M. Gragnaniello, et al., "Edge-AI on Wearable Devices: Myocardial Infarction Detection with Spectrogram and 1D-CNN," in Proc. IEEE MELECON, pp. 485-490, 2024. https://doi.org/10.1109/MELECON56669.2024.10608624

[9] P. Prabhakar, P. B. Pati, and S. Parida, "Navigating Legal and Ethical Dimensions in AI, IoT, and Cloud Solutions for Women's Safety," in Developing AI, IoT and Cloud Computing-based Tools and Applications for Women's Safety, pp. 155-191, Chapman & Hall/CRC, 2025. https://doi.org/10.1201/9781003538172-11

[10] N. M. Kruthika, S. Kavipriya, and P. B. Harshini, "Development of Women's Safety System Using IoT and Taser Technology," in Proc. 4th Asian Conf. Innovation Technol. (ASIANCON), pp. 1-6, IEEE, 2024.
https://doi.org/10.1109/ASIANCON62057.2024.10837901
[11] K. Tamilarasi, R. T., B. Madhumitha, and S. Shruthi, "Women Safety Analytics," in Proc. Int. Conf. Syst., Comput., Autom. Netw. (ICSCAN), pp. 1-6, 2024.
https://doi.org/10.1109/ICSCAN62807.2024.10894051
[12] Randhave and Rawas, "IoT Based Women Safety Devices with Screaming Detection and Photo Capturing," Int. Res. J. Adv. Eng. Manage., 2025.
https://doi.org/10.55041/IJSREM50006
[13] M. Mishra, "Women Hawk," Int. J. Sci. Res. Eng. Manage. (IJSREM), vol. 5, no. 1, pp. 1–5, Jan. 2025.
[14] Khanum and Kumawat, "Intelligent Voice and Emotion Recognition for Women's Safety: An IoT-Enabled Wearable Emergency System," in Proc. Int. Conf. Electron. Renewable Syst. (ICEARS), pp. 758-766, 2025.
https://doi.org/10.1109/ICEARS64219.2025.10941429
[15] N. Alharbe and M. Almalki, "IoT-enabled healthcare transformation leveraging deep learning for advanced patient monitoring and diagnosis," Multimedia Tools Appl., 2024.
https://doi.org/10.1007/s11042-024-19919-w
[16] S. Bijapur and S. Bhanuse, "The Role of IoT in Woman's Safety: A Systematic Literature Review," Int. J. Adv. Res. Sci., Commun. Technol. (IJARSCT), vol. 5, no. 2, pp. 2080–2086, Feb. 2025.
[17] Al, et al., "An IoT-based Women's Safety Threat Detection using a Temperature Sensor," J. Netw. Commun. Syst., vol. 8, no. 1, 2025.
https://doi.org/10.46253/jnacs.v8i1.a2
[18] Bai and Bai, "A Systematic Survey on IoT-Based Devices for Enhancing Women's Safety," Int. J. Eng. Res. Sci. Technol., vol. 21, no. 2, pp. 712-722, 2025.
https://doi.org/10.62643/ijerst.2025.v21.i2.pp712-722
[19] Afranaaz and M. Basthikodi, "Enhancing Women's Safety - A Comprehensive Review of Emerging Technologies and Automated Crime Detection Using ML/DL Algorithms," in Proc. Int. Conf. Comput., Semicond., Mechatronics, Intell. Syst. Commun. (COSMIC), pp. 1-8, 2024.
https://doi.org/10.1109/COSMIC63293.2024.10871586
[20] D. H. Hussein, Y. M. Ismail, S. Askar, and M. A. Ibrahim, "Integration of Deep Learning Applications and IoT for Smart Healthcare," Indones. J. Comput. Sci., vol. 14, no. 1, 2025.
https://doi.org/10.33022/ijcs.v14i1.4611
[21] P. S. Bharathi, T. Judgi, D. Pradeep, A. T. S., A. A. A. Samhan, and J. Giri, "A Novel Internet Of Things (IoT) Enabled Women Safety System Design with Emergency Alert Mechanism," in Proc. Int. Conf. Frontier Technol. Solutions (ICFTS), Chennai, India, 2025, pp. 1-7.
https://doi.org/10.1109/ICFTS62006.2025.11031774
[22] K. Chaudhary, P. Singh, and H. S. Dev, "Smart Safety Solutions: Utilizing MobileNet v2 for Violence Recognition to Enhance Women's Safety," in Proc. 6th Int. Conf. Emerg. Technol. (INCET), Belgaum, India, 2025, pp. 1-7.
https://doi.org/10.1109/INCET64471.2025.11139972
[23] R. Singh, M. Kaur, and N. Kumar, "Edge AI: A survey," Eng. Appl. Artif. Intell., vol. 122, 2023, Art. no. 106085.
[24] D. Saha, A. K. Mondal, and S. Das, "Real-time deployment of MobileNetV3 model in edge computing devices," Appl. Sci., vol. 13, no. 13, p. 7804, 2023.
https://doi.org/10.3390/app13137804
[25] C. V. F. Pereira, A. A. Lopes, and L. A. Alexandre, "Machine learning applied to edge computing and wearable devices in healthcare: A systematic mapping," Sensors, vol. 24, no. 13, p. 4277, 2024.
https://doi.org/10.3390/s24196322